

Kinetics and mechanism of the oxidation of water soluble porphyrin Fe^{III}TPPS with hydrogen peroxide and the peroxomonosulfate ion†

Gábor Lente* and István Fábrián

Received 13th June 2007, Accepted 9th July 2007

First published as an Advance Article on the web 2nd August 2007

DOI: 10.1039/b708961a

The overall six-electron oxidation of water soluble porphyrin Fe^{III}TPPS by hydrogen peroxide and peroxomonosulfate ion was studied by the stopped-flow method with UV-vis detection. A three-step consecutive reaction was observed with two intermediates: Fe^{III}TPPS → Int₁ → Int₂ → products. The products were identified as the iron(III) complex of the biliverdin analog formed from TPPS and 4-sulfobenzoic acid. All the rate constants with both oxidizing agents were determined. Intermediate Int₁ is proposed to be the species (TPPS^{•+})Fe^{IV}=O. Although no unambiguous proposal for the structure of Int₂ can be made, it is most probably the product of the four-electron oxidation of the original Fe^{III}TPPS, contains an iron-oxo center and has a dissociable proton with a p*K* of around 3.1. In spite of the protolytic equilibria occurring in the pH region 2–4, the kinetic observations do not show pH dependence.

Introduction

High-valent iron compounds appearing as intermediates in catalytic oxidation cycles have been studied very intensively recently.^{1–9} These studies are usually inspired by both the widespread practical catalytic applications of iron complexes and the important biochemical role iron plays in heme and non-heme enzymes. In order to characterize the structure of high-valent iron intermediates thoroughly, it is usually necessary to stabilize them, *e.g.* by lowering the temperature or clever selection of solvent and/or ligand used. Independent efforts should be devoted to

confirming that the stabilized and structurally studied compounds are the same as the intermediates appearing in actual catalytic or biochemical processes, which usually occur in aqueous solution at around room temperature. One possible strategy to resolve this problem, which has been used in some earlier reports,^{10,11} requires detailed kinetic studies of the corresponding processes under conditions that are catalytically relevant. These investigations could provide at least indirect information on the reactivities of the intermediates involved and the kinetic role of the structurally characterized ‘stabilized intermediates’.

Our interest in the destructive chemical oxidation of chlorophenols^{12–16} by H₂O₂ led us to study the water soluble porphyrin Fe^{III}TPPS (formula is given in Chart 1), which is an efficient catalyst in this process.^{14–16} A careful approach to exploring the mechanism of the catalysis should begin with studying independently all the possible subsystems of the three-component chlorophenol–H₂O₂–catalyst system. Chlorophenols

University of Debrecen, Department of Inorganic and Analytical Chemistry, Debrecen 10, P.O.B. 21, Hungary, H-4010. E-mail: lented@delfin.unideb.hu; Fax: +36 52 489-667; Tel: +36 52 512-900/22373

† Electronic supplementary information (ESI) available: kinetic traces of the reactions; ESI-MS of reactants and products; mathematical background to eqn (4). See DOI: 10.1039/b708961a

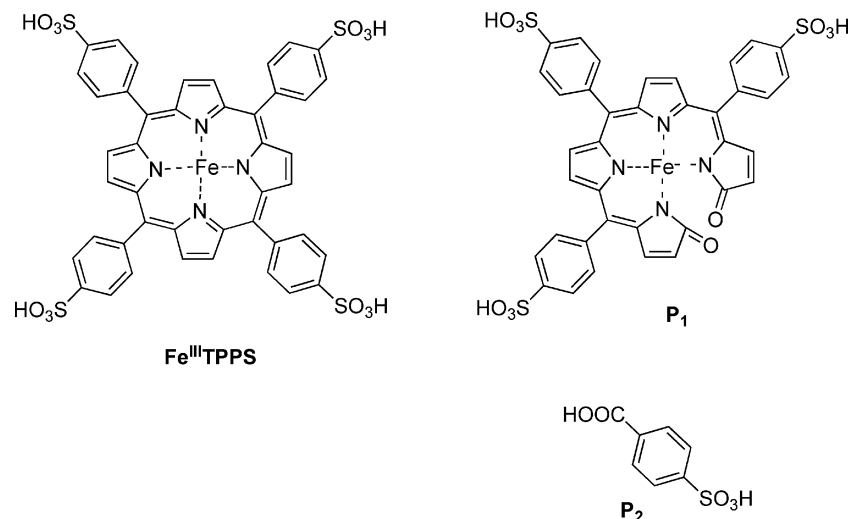


Chart 1

do not react with H_2O_2 directly (hence the need for a catalyst), and our results indicated that $\text{Fe}^{\text{III}}\text{TPPS}$ does not interact directly with chlorophenols, either. Therefore, the chain of catalytic events must start with the reaction between $\text{Fe}^{\text{III}}\text{TPPS}$ and H_2O_2 . This reaction is highly important because it is in the core of the catalytic process, but it may also result in irreversible oxidation, and as a consequence, inactivation of the catalyst. Ultimately, the interplay of these somewhat counteracting processes determines the efficiency of the catalyst.

Although results on many iron porphyrin catalyzed oxidation reactions have already been published,^{17–23} exploring the reaction between the catalyst and the oxidant without any third reagents has not received the attention it deserves. A notable exception is an earlier study on the direct reaction of $\text{Fe}^{\text{III}}\text{TPPS}$ with H_2O_2 in slightly basic solution.²¹ These results are not very relevant with respect to catalytic activity because, under these conditions, $\text{Fe}^{\text{III}}\text{TPPS}$ exists exclusively as an oxo-bridged dimer^{24,25} with diminished reactivity.²¹ In addition, more data are available for the reactions of different iron porphyrins with alkyl-peroxide oxidizing agents in non-aqueous solvents,^{26,27} but the results of these studies are not directly transferable to aqueous conditions. In this paper, we report our detailed mechanistic studies on the $\text{Fe}^{\text{III}}\text{TPPS}$ – H_2O_2 reaction in aqueous solution and in the absence of any oxidizable reagents under conditions where the monomeric parent complex dominates ($\text{pH} < 7$). Detailed experiments with another peroxide type oxidant, peroxomonosulfate ion (HSO_5^-), were also carried out in both the absence and presence of an oxidizable chlorophenol in order to draw more convincing mechanistic conclusions.

Experimental

Materials

$\text{Fe}^{\text{III}}\text{TPPSCl}$ was purchased from Frontier Scientific. The iron content of a $\text{Fe}^{\text{III}}\text{TPPSCl}$ stock solution (25.3 mg dm^{-3}) was measured by ICP-AES to be $23.0 \pm 1.0 \text{ } \mu\text{M}$ in acceptable agreement with the calculated value ($24.7 \text{ } \mu\text{M}$), which confirmed that the sample was of sufficient purity. Hydrogen peroxide stock solutions were standardized by permanganometry every day. H_2O_2 -containing samples were prepared freshly before use. Potassium peroxomonosulfate stock solutions were prepared every day from oxone ($2\text{KHSO}_5 \cdot \text{KHSO}_4 \cdot \text{K}_2\text{SO}_4$, Aldrich) and standardized by iodometric titration. In this case, it was confirmed that the chloride content of $\text{Fe}^{\text{III}}\text{TPPSCl}$ did not interfere with the measurements as chloride ion is oxidized by HSO_5^- , much slower (several hours) than the metal complex (less than a minute). Perchloric acid was used as a strong acid to set the pH, the ionic strength was set with NaClO_4 , which was prepared as described earlier.²⁸ Extra care was taken to make sure that the oxidant concentration is sufficiently low to avoid the precipitation of KClO_4 in the case of oxone, which contains K^+ ions. All other chemicals used in this study were of analytical reagent grade and purchased from commercial sources. Doubly deionized and ultrafiltered water from a Millipore Q system was used to prepare the stock solutions and samples.

Instrumentation and computation

UV-vis spectra and kinetic curves were recorded on Perkin Elmer Lambda 25 or Perkin Elmer Lambda 2 S scanning, and HP-8543

diode-array spectrophotometers. Fast kinetic measurements were performed with an Applied Photophysics DX-17 MV sequential stopped-flow apparatus using 1 cm optical path length. The dead time of the instrument was measured to be $1.09 \pm 0.02 \text{ ms}$ by published methods.^{29,30} In some experiments, an Applied Photophysics PD.1 Photodiode Array accessory was used as a detector of the stopped-flow instrument. Quantitative kinetic measurements were also performed in the HP-8543 diode-array spectrophotometer using an RX-2000 Applied Photophysics Rapid Kinetics Accessory. A YSI 5100 Dissolved Oxygen Meter and a YSI Model 5239 probe with YSI 5906 membrane cap were used for measuring the concentration of dissolved oxygen in aqueous solutions. In some experiments, a Weiss Research CL3005 combination chloride ion selective electrode was used (constant ionic strength maintained with 0.10 M NaNO_3) connected to a Hanna Instruments pH302 pH-meter. A GK2401C combination glass electrode was used to measure pH attached to radiometer PHM85 pH-meter. The pH-meter reading was converted into $\log[\text{H}^+]$.³¹ Mass spectrometric analysis was performed by a Bruker micrOTOF-Q instrument with electrospray ionization in the negative ion mode. The software SCIENTIST,³² ZiT_a,³³ and Matlab³⁴ were used in the fitting procedures.

Results

Spectral observations

When $\text{Fe}^{\text{III}}\text{TPPS}$ is mixed with H_2O_2 or HSO_5^- in acidic solution, the intense color of the iron complex fades. The Soret band of the porphyrin ring disappears showing that the complex is oxidized to a product that does not have a porphyrin ring. A series of time resolved UV-vis spectra recorded during the reaction of $\text{Fe}^{\text{III}}\text{TPPS}$ with H_2O_2 is shown in Fig. 1. Isosbestic points detectable at early reaction times (at about 360, 440, 510, and 550 nm) disappear giving unambiguous evidence that a multistep redox process is observed.

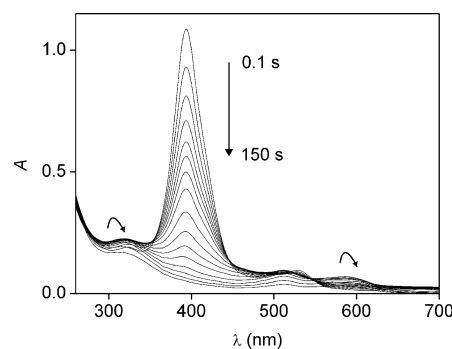


Fig. 1 Spectral observations during the reaction of $\text{Fe}^{\text{III}}\text{TPPS}$ with H_2O_2 . $[\text{Fe}^{\text{III}}\text{TPPS}] = 9.5 \text{ } \mu\text{M}$; $[\text{H}_2\text{O}_2] = 13.2 \text{ mM}$; $\text{pH} = 3.05$; optical path length = 1.00 cm ; $T = 25.0 \text{ } ^\circ\text{C}$; $I = 0.1 \text{ M (NaClO}_4)$; reaction times: increasing time intervals from 0.1 s to 150 s.

The kinetic curves recorded at 520 nm at varying pH in the range 3.7–2.1 clearly demonstrate that the observations are pH-dependent (Fig. 2). The origin of this pH effect will be explained later. Four of the five kinetic curves in Fig. 2 show an absorbance decrease first, then an increase for some time, and finally a decrease again. Therefore, both a minimum and a maximum are present in

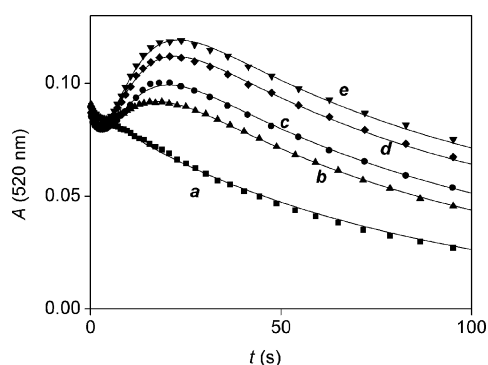


Fig. 2 Kinetic traces during the reaction of Fe^{III}TPPS with H₂O₂. [Fe^{III}TPPS] = 9.5 μM; [H₂O₂] = 13.2 mM; pH = 3.68 (a), 3.05 (b), 2.76 (c), 2.37 (d), 2.16 (e); λ = 520 nm; optical path length = 1.00 cm; T = 25.0 °C; I = 0.1 M (NaClO₄). Solid lines are fitted curves using eqn (1).

each of these curves, which unambiguously prove that the studied reaction sequence includes at least two intermediates and at least three consecutive reaction steps. The oxidizing agent was used in a large (usually more than 100-fold) excess in all experiments, therefore its concentration does not change during the process and multiexponential curves are expected to be seen if all the reactions are first order with respect to Fe^{III}TPPS and the intermediates.³⁵ In agreement with this expectation, kinetic traces with both oxidizing agents gave an excellent fit to a treble exponential curve:

$$A = A_1 e^{-k_{\text{obs}1} t} + A_2 e^{-k_{\text{obs}2} t} + A_3 e^{-k_{\text{obs}3} t} + E \quad (1)$$

The lines in Fig. 2 show the best fits for curves recorded with H₂O₂ as an oxidizing agent, Fig. 3 shows a kinetic curve recorded with the HSO₅⁻ ion and the best fit to a treble exponential function. With H₂O₂, the oxidation proceeded without giving well separated phases on the time scale of a few minutes. With HSO₅⁻, the reaction was faster, usually complete in about 20 s and the first phase of the process was separate from the other two overlapping phases. As expected, fitting the first phase only (up to about 50 ms) with a single exponential function gave, within experimental error, the same pseudo first order rate constants as the fastest one from the treble exponential fits. The absorbance change associated with this first phase could be determined in stopped-flow studies using the PD.1 diode-array detector with a wavelength resolution of 2.5 nm.

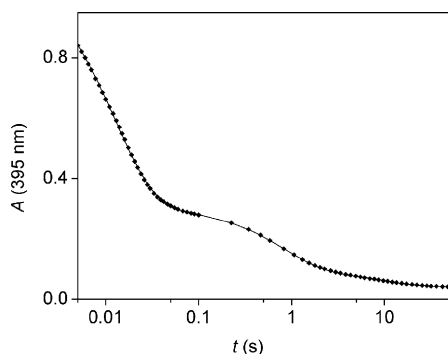


Fig. 3 Comparison of experimental (markers) and fitted treble exponential (line) kinetic traces during the reaction of Fe^{III}TPPS with HSO₅⁻. [Fe^{III}TPPS] = 6.9 μM; [HSO₅⁻] = 3.9 mM; pH = 1.30; λ = 395 nm; optical path length = 1.00 cm; T = 25.0 °C; I = 0.1 M (NaClO₄); only a selection of measured points (~ 7%) is shown and logarithmic time scale is used for clarity.

The same was not possible for H₂O₂, where the first phase was not separate, but initial rates could be obtained as a function of wavelength. After normalization, which means division of each value with the largest absolute value in a given series of data, the comparison of these two quantities leads to an important conclusion (Fig. 4, Fig. S1 in the ESI† shows the vis part of the same graph with an expanded y axis). The wavelength dependences of the two quantities are very similar, clearly suggesting that the same absorbing species are involved in the first phase in both cases and the Fe^{III}TPPS is initially oxidized to the same absorbing intermediate by both H₂O₂ and HSO₅⁻.

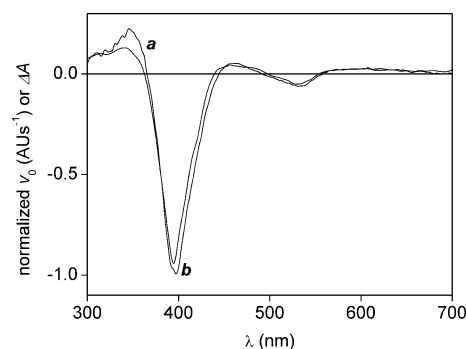


Fig. 4 Comparison of normalized absorbance changes for the first phase (a, with HSO₅⁻) and normalized initial rates (b, with H₂O₂) as a function of wavelength during the reaction of Fe^{III}TPPS with HSO₅⁻ and H₂O₂. [Fe^{III}TPPS] = 6.9 μM (a), 9.5 μM (b); [HSO₅⁻] = 2.95 mM (a); [H₂O₂] = 8.77 mM (b); pH = 1.30 (a), 3.05 (b); optical path length = 1.00 cm; T = 25.0 °C; I = 0.1 M (NaClO₄).

In some experiments, a diode array spectrophotometer was used for detection. It is well known that the light of a diode-array instrument has relatively high intensity and can induce photochemical reactions.¹³ In fact, the instrument can be used as a photochemical device for certain purposes,^{36,37} and neglecting the possible effect of light of a diode array spectrophotometer led to seriously erroneous conclusions in some cases.^{38,39} As porphyrins absorb light strongly and have widespread photochemistry,^{40,41} we took precautions to avoid interference from photochemical processes. When the diode-array spectrophotometer was used for detection, the time of illumination was the shortest possible. In a few cases, the same experiments were carried out with longer overall illumination times as well. Because the kinetic curves did not depend on the time of illumination, it could be concluded that photochemical processes do not interfere detectably with the oxidation process under our conditions.

Quantitative kinetic results: concentration dependence

First, initial rates were measured in the reaction between Fe^{III}TPPS and H₂O₂. The initial rate showed first order dependence on the concentrations of both H₂O₂ and Fe^{III}TPPS (Fig. S2 and S3 in ESI†).

The kinetic curves could be fully analyzed through the three pseudo first order rate constants, $k_{\text{obs}1}$, $k_{\text{obs}2}$, and $k_{\text{obs}3}$ determined in each experiment. In the case of H₂O₂, it was not possible to find a wavelength that was sensitive enough for all of the three phases (*i.e.* at least one of them was accompanied by a minor absorbance change at any given wavelength). However, it was

possible to extract the three pseudo first order rate constants from multiwavelength data using global analysis.⁴² In this approach, kinetic curves measured at 81 wavelengths (from 300 to 700 nm with an interval of 5 nm) were fitted simultaneously to treble exponential curves that could have different amplitudes for each wavelength but had the same pseudo first order rate constants. Fig. 5 shows the dependence of k_{obs1} and k_{obs2} on the concentration of H_2O_2 . It is clear that k_{obs1} is directly proportional to the oxidant concentration:

$$k_{\text{obs1}} = k_1^{\text{H}}[\text{H}_2\text{O}_2] \quad (2)$$

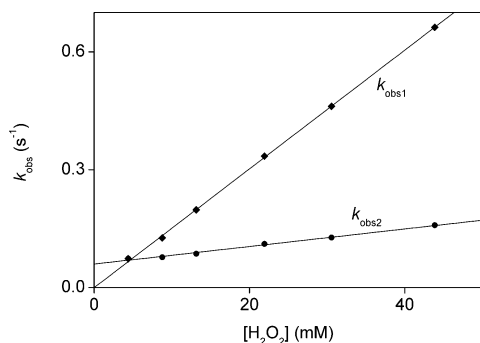


Fig. 5 Dependence of pseudo first order rate constants k_{obs1} and k_{obs2} on the oxidant concentration during the reaction of Fe^{III} TPPS with H_2O_2 . [Fe^{III} TPPS] = 9.5 μM ; pH = 3.05; T = 25.0 $^{\circ}\text{C}$; I = 0.1 M (NaClO_4).

Linear least squares fitting yielded the second-order rate constant $k_1^{\text{H}} = 15.1 \pm 0.1 \text{ M}^{-1} \text{ s}^{-1}$. Fig. 5 shows that k_{obs2} depends on the oxidant concentration linearly, but there is a significant intercept. Therefore, the corresponding equation is

$$k_{\text{obs2}} = k_{2a}^{\text{H}}[\text{H}_2\text{O}_2] + k_{2b}^{\text{H}} \quad (3)$$

Parameters $k_{2a}^{\text{H}} = 2.23 \pm 0.09 \text{ M}^{-1} \text{ s}^{-1}$ and $k_{2b}^{\text{H}} = 0.060 \pm 0.002 \text{ s}^{-1}$ were resolved by the least squares fitting procedure.

It should be noted that k_{obs1} and k_{obs2} are very close at the lowest H_2O_2 concentration shown in Fig. 5. In fact, it was not possible to fit the experimental kinetic curves measured at this point to a treble exponential function. This is not very surprising as the analytical solution of the linear, first order differential equation for the special case $k_{\text{obs1}} = k_{\text{obs2}}$ is not a treble exponential function as given in eqn (1). The solution contains a term which is composed of a polynomial of the independent variable (t) multiplied with an exponential function. The correct mathematical form is (see more detailed mathematical background on pages S11–S12 of ESI†):

$$A = (A_1 + A_2 t)e^{-k_{\text{obs1}} t} + A_3 e^{-k_{\text{obs3}} t} + E \quad (4)$$

The value of $k_{\text{obs12}} = k_{\text{obs1}} = k_{\text{obs2}}$ was fitted using eqn (4) for this special case.

The third pseudo first order rate constant, k_{obs3} of the process depended linearly on the oxidant concentration (Fig. S4 in ESI†):

$$k_{\text{obs3}} = k_{3a}^{\text{H}}[\text{H}_2\text{O}_2] + k_{3b}^{\text{H}} \quad (5)$$

The values $k_{3a}^{\text{H}} = 0.30 \pm 0.03 \text{ M}^{-1} \text{ s}^{-1}$ and $k_{3b}^{\text{H}} = (7.6 \pm 0.6) \times 10^{-3} \text{ s}^{-1}$ were determined.

As already noted, the first phase of the reaction was separate from the others during the oxidation with HSO_5^- . Quantitative measurements were carried out at a single wavelength by the stopped-flow method. The 395 nm Soret band of Fe^{III} TPPS

was sensitive for all three phases of the reaction in this case. Therefore, all three rate constants could be determined from treble exponential kinetic curves measured at 395 nm. All three observed rate constants were directly proportional to the concentration of the oxidant (Fig. S5–S7 in ESI†):

$$k_{\text{obs1}} = k_1^{\text{S}}[\text{HSO}_5^-] \quad (6)$$

$$k_{\text{obs2}} = k_2^{\text{S}}[\text{HSO}_5^-] \quad (7)$$

$$k_{\text{obs3}} = k_3^{\text{S}}[\text{HSO}_5^-] \quad (8)$$

The second-order rate constants $k_1^{\text{S}} = (2.00 \pm 0.02) \times 10^4 \text{ M}^{-1} \text{ s}^{-1}$, $k_2^{\text{S}} = (3.67 \pm 0.05) \times 10^2 \text{ M}^{-1} \text{ s}^{-1}$, and $k_3^{\text{S}} = (2.85 \pm 0.05) \times 10^1 \text{ M}^{-1} \text{ s}^{-1}$ were determined by least squares fitting.

Quantitative kinetic results: pH dependence

Fe^{III} TPPS is known to form an oxo-bridged dimer above pH 7,^{24,25} which was shown to be catalytically inactive in the H_2O_2 dependent oxidation of chlorophenols.¹⁴ In this work, it was further confirmed that the oxo bridged dimer $\text{TPPSFe}^{\text{III}}\text{--O--Fe}^{\text{III}}$ TPPS does not react with H_2O_2 . In experiments carried out in phosphate buffer at pH ~ 7.2 , no spectral changes were detected for about 60 min upon the addition of H_2O_2 to a sample of Fe^{III} TPPS. Iodometric titrations also confirmed that no significant amount of the oxidant is lost over a few hours in the same reaction.

In view of these findings, the present study was limited to the acidic pH range. Concern about possible interference of buffers¹⁶ (complexation or oxidation) led us to avoid using them at all. Therefore, the pH was set with strong acid (usually perchloric acid) only and no experiments were carried out in the 4.5–6 pH range. The initial rate was measured in the reaction with H_2O_2 and it was independent of pH in the entire pH region studied (1.8–3.8, Fig. S8 in ESI†). Similarly to the spectral comparison shown in Fig. 4, the initial rates measured at several different wavelengths were also compared between experiments at pH = 2.16 and 3.05 (Fig. S9 in ESI†). The same curve was obtained, therefore the pH did not influence the formation rate or the identity of the product in the first phase. The pseudo first order rate constants determined in a series of experiments from the analysis of full curves did not show any pH-dependence, either. At first sight, this may seem to contradict the fact that different kinetic traces were measured at different pH values as shown in Fig. 2. However, the curves in Fig. 2 give identical pseudo first order rate constants and only the amplitudes A_2 and A_3 are significantly different. This implies that the spectrum and most probably the identity of an intermediate changes in this pH range (1.8–3.8), but the rate constants remain the same. This unexpected phenomenon will be discussed in more detail in the next sections. In the case of HSO_5^- , experiments were carried out in the pH range 0.5–2, and the kinetic curves did not depend on the pH in this range (Fig. S10 in ESI†). The absence of a kinetic pH effect can be rationalized easily: no significant acid–base equilibria involving any of the reagents, H_2O_2 , HSO_5^- , and Fe^{III} TPPS occur in the pH range of the present study. It follows that if the reactions occur between the dominant species, no pH-dependence arises.

Stoichiometric observations

It is well known that the biochemical pathway of porphyrin degradation yields biliverdin and carbon monoxide.⁴³ We note that this oxidation scheme is an overall six electron oxidation or three consecutive oxygen transfer steps. This suits nicely our kinetic observations, which showed that a three-step process is operative. Thus, it was assumed that the products of the oxidation of Fe^{III}TPPS are the iron(III) complex of the biliverdin analog formed from TPPS (P₁ in Chart 1) and a carboxylic acid (P₂ in Chart 1), which is the analog of carbon monoxide when the carbon atom in the porphyrin ring has a substituent.

It was noted that some acid is formed in the oxidation reaction in unbuffered solution. Experiments were designed to study the stoichiometry of this acid production: the pH of an unbuffered solution was followed after the addition of H₂O₂ to Fe^{III}TPPS. Fig. 6 shows the pH as a function of time. In the beginning, the sample is slightly acidic because Fe^{III}TPPS has four strongly acidic sulfonic acid groups which are ionized completely. The pH decreases as the reaction progresses, and the concentration of acid formed can be calculated for each point from the measured data. These experiments showed that approximately one equivalent acid is formed per Fe^{III}TPPS, which means that the final amount of extra acid equals the initial amount of Fe^{III}TPPS. The sulfonic acid groups are conserved without modification during the reaction and remain ionized. Therefore, they cannot be responsible for acid production. The source of acidification is sulfobenzoic acid P₂, in which the carboxylic group is newly formed as a result of the oxidation reaction. Independent literature data show that this carboxylic acid has a pK_a of 3.65,⁴⁴ and it is mostly ionized at the final pH of the experiment shown in Fig. 6. These considerations are in agreement with the production of a single equivalent of acid in the reaction. Similar pH-metric experiments were not possible with the HSO₅⁻ ion because the reagent used to prepare the solutions, oxone, also contains HSO₄⁻ ions, the dissociation of which produces further acid, and makes reliable quantitative stoichiometric studies difficult to perform.

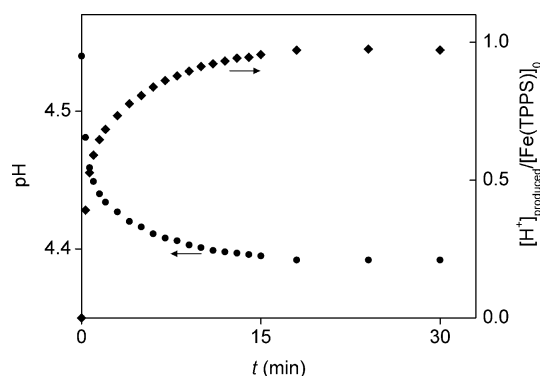


Fig. 6 The change in pH (left axis) and the amount of acid produced (right axis) during the reaction of Fe^{III}TPPS with H₂O₂. [Fe^{III}TPPS] = 17.3 μM; [H₂O₂] = 25 mM; T = 25.0 °C; I = 0.2 M (KCl).

Further identification of reaction products was attempted with ESI mass spectroscopy in negative ion mode. The oxidation reaction was driven to completion by adding about 5 equivalents of HSO₅⁻ to a solution of Fe^{III}TPPS at about pH 1, and the final solution was analyzed. As shown in Fig. 7, the sets of MS peaks

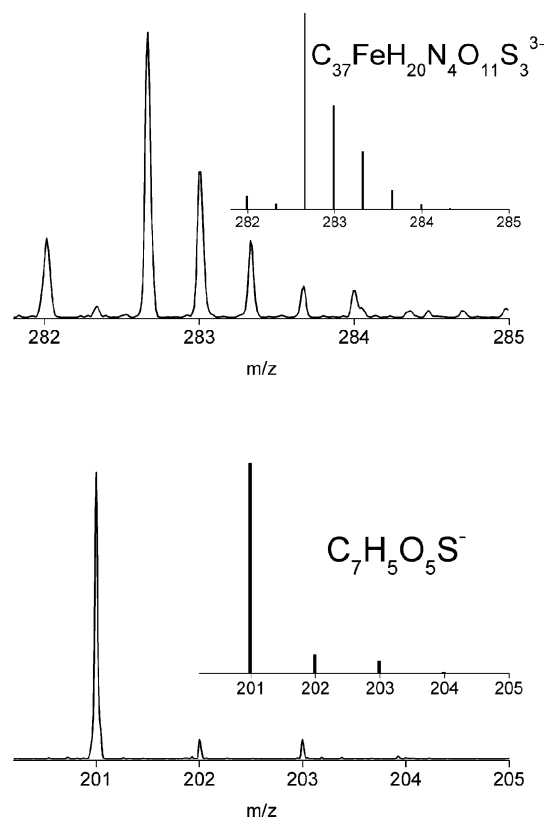


Fig. 7 ESI mass spectra of the products formed in the reaction of Fe^{III}TPPS with HSO₅⁻. Large graphs are the measured spectra, insets are simulated spectra for the ion with the composition shown. The spectra are consistent with the formula of P₁ and P₂ (Chart 1).

characteristic of the ions C₃₇FeH₂₀N₄O₁₁S₃³⁻ (the dominant form of P₁ at pH = 1) and C₇FeH₅O₅S⁻ (the dominant form of P₂ at pH = 1) were both clearly recognizable. This lends strong support to our assumed stoichiometry, and together with the quantitative pH measurements and the clean kinetic observations, confirms that no other significant products are formed during the reaction.

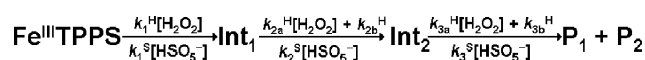
When the oxidants were used in larger excess, slow further reactions were also observed. These may have involved further oxidation of P₁ or P₂, but were too slow to interfere with our kinetic measurements.

Spectrophotometric titration was also attempted to establish the oxidant/Fe^{III}TPPS stoichiometric ratio experimentally. However, these experiments remained inconclusive. In the case of the reaction with H₂O₂, clear evidence was obtained that decomposition of H₂O₂ to water and oxygen also occurs. This was confirmed by experiments with a dissolved oxygen electrode, which showed a slight increase in oxygen concentration during the reaction. Therefore, H₂O₂ is consumed in two different reactions and it is not possible to characterize the stoichiometry of one of them alone. The loss of H₂O₂ was negligible compared to the initial concentration during the kinetic runs. Thus, pseudo first order conditions were maintained in all kinetic experiments. The dissolved oxygen electrode experiments also proved that O₂ does not have a significant role in the process as an oxidant because its concentration did not decrease. Evidence for some catalytic oxidant decomposition was also obtained in the experiments with HSO₅⁻ as the spectral observations during titrations were

dependent on the increment size of oxidant addition and not only on the amount of oxidant totally added.

Discussion

As shown in the previous sections, Fe^{III}TPPS is oxidized in a consecutive three-step process which can be represented by the simple series of reactions shown in Scheme 1. The fact that the detected curves are treble exponential proves that the first, second, and third reactions are first order with respect to Fe^{III}TPPS, Int₁, and Int₂, in order. It is well known that the fastest pseudo first order rate constant obtained from the treble exponential fit does not necessarily correspond to the first reaction step in Scheme 1.³⁵ The assignment of rate constants to reactions should always be based on independent considerations. Usually, the values of the molar absorbances required by a particular assignment provide a good way to do this because assignments requiring unreasonably high molar absorbances can be ruled out.³⁵



Scheme 1

For HSO₅⁻, it was confirmed that the fast pseudo first order rate constant belongs to the first step, the middle rate constant to the second step, the slow rate constant to the third step. Any other assignment led to impossibly high (>>10⁸) molar absorbances for one or both of the intermediates Int₁ and Int₂. Similar considerations showed that the slow rate constant must correspond to the third step in the case of H₂O₂, but the first two could not be assigned on the basis of similar considerations (Fig. 5 shows that *k*_{obs1} and *k*_{obs2} are usually close to each other). A different method was used to clarify this problem: the second-order rate constant calculated from the initial rates was compared with *k*₁^H calculated from the dependence of *k*_{obs1} on the concentration of H₂O₂. The two values agreed within experimental error showing that *k*_{obs1} corresponds to the first step. It follows that *k*_{obs2} belongs to the second reaction step in the sequence. It should be noted that this order (fastest phase is first, middle phase is second) can change at low oxidant concentration, as also apparent from Fig. 5.

It was shown in a previous section that the identity of the intermediate Int₁ does not depend on whether HSO₅⁻ or H₂O₂ is used as an oxidant. This fact has important consequences for proposing a structure for Int₁. When H₂O₂ is the oxidant, it would be natural to assume that an end-on hydroperoxo complex, TPPSFe^{III}-OOH,⁵ forms at first, the decomposition of which can give rise to a species with a higher oxidation state metal center. However, formation of the hydroperoxo complex seems rather unlikely when HSO₅⁻ is used as the oxidant. Since the two processes have the same detectable intermediates, the hydroperoxo complex cannot be a spectroscopically detectable intermediate in the reaction with H₂O₂, although it may still be a steady-state intermediate whose concentration is not high enough to be detected. Thus, Int₁ is most likely a formally iron(v) oxo species, which is often postulated to form in catalytic redox cycles containing porphyrins.^{17-23,45-48} The actual structure of this species is thought to be iron(IV) oxo with one electron removed from the porphyrin ring as well, (TPPS⁺)Fe^{IV}=O.^{45,46}

It is much more difficult to make a reasonable proposal for the structure of Int₂. This species is the product of the two electron oxidation of Int₁. Analysis of spectral data showed that the absorbance contribution of Int₂ is rather significant above 500 nm. Therefore, once the assignment of rate constants to processes was successful, the UV-vis spectrum of Int₂ could be resolved with acceptable precision in this wavelength region. Fig. 8 shows the resolved molar absorption spectra of Int₂ at 6 different pH values. The spectrum of Int₂ seems to depend on pH quite strongly. This explains the earlier observation that the amplitudes of the fitted treble exponential functions depend on the pH whereas the rate constants do not (see Fig. 2). The pH variation of spectra shown in Fig. 8 can be readily interpreted by assuming that Int₂ contains a dissociable proton. Data measured at 15 different wavelengths were simultaneously fitted to the following equation:

$$\varepsilon_i = \frac{e_i^{\text{Int}_2} K + e_i^{\text{HInt}_2} [\text{H}^+]}{K + [\text{H}^+]} \quad (9)$$

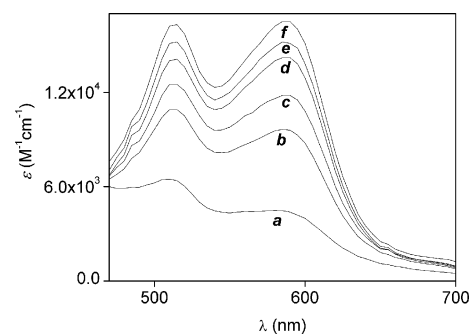


Fig. 8 pH dependence of the absorption spectrum of intermediate Int₂ formed during the reaction of Fe^{III}TPPS with H₂O₂. pH = 3.68 (a), 3.05 (b), 2.76 (c), 2.37 (d), 2.16 (e), 1.95 (f); T = 25.0 °C; I = 0.1 M (NaClO₄).

In eqn (9), *K* is the acid dissociation constant of Int₂. The fitting gave p*K* = 3.08 ± 0.02, and showed that the protonated form of Int₂, which dominates in more acidic solution, has stronger absorption above 500 nm. The value of the fitted p*K* also explains why the shape of the kinetic curves did not depend on pH in the case of HSO₅⁻, where the pH range was narrower (0.5–2). It is interesting to note that although this protonation/deprotonation influences the spectral properties of Int₂ significantly, there is no detectable effect on the reactivity, *i.e.* the two forms seem to react with the oxidizing agent at basically the same rates. This might imply that the dissociable proton could be far from the site where the oxidant attacks Int₂.

As noted previously, the pseudo first order rate constants measured in the HSO₅⁻ system were directly proportional to the oxidant concentration. The same was not true for the H₂O₂ system, where the dependences of *k*_{obs2} and *k*_{obs3} on the oxidant concentration were linear but showed rather significant intercepts. These intercepts imply that the oxidation of Int₁ to Int₂ and the oxidation of Int₂ to P₁ and P₂ can also proceed *via* a pathway where H₂O₂ only attacks after the rate determining steps. These pathways are simple first-order reactions of Int₁ and Int₂, and consequently must be present in the HSO₅⁻ system as well. However, their contribution to the overall rate is negligible because the direct reaction with the oxidant is much faster here. In the case of Int₁, it is easy to imagine a process in which the oxo group on the iron

center is transferred to some part of the porphyrin ring without the assistance of an oxidant molecule, and the resulting species is oxidized by H_2O_2 quite rapidly to give Int_2 . A similar sequence of steps is only possible in the oxidation of Int_2 if it contains an iron-oxo center. This may suggest that the structure of Int_2 contains a high-valent iron-oxo center and a hydroxyl group, which might be responsible for the pK observed. A possible, though clearly speculative structure that interprets all the listed features for Int_2 is shown in Chart 2. We note that further structural characterization of Int_2 does not seem to be feasible as it has a fast first-order decay (0.5 min^{-1}) even when no oxidizing agent is present and always coexists with Int_1 and the products. Compounds similar to α -*meso*-hydroxyheme, which are often implied as intermediates in heme metabolism,^{47,48} cannot be intermediates in this system because there are no hydrogens in Fe^{III} TPPS in a suitable position to form them.

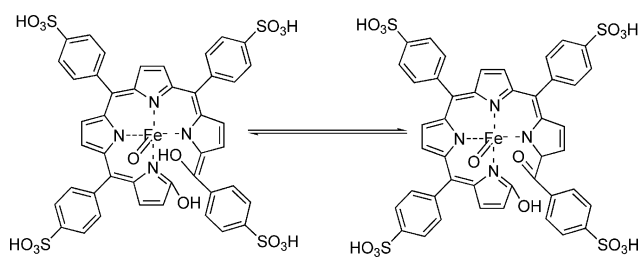


Chart 2

To conclude this study, control experiments were designed to test the relevance of the results in Fe^{III} TPPS catalyzed oxidation of 2,4,6-trichlorophenol (TCP) with HSO_5^- . The process was first followed using a chloride ion selective electrode. The reaction produced one equivalent of chloride ion within a minute (Fig. S11 in ESI†) and further production of Cl^- was not observed at longer reaction times. UV-vis spectra confirmed that the primary oxidation product with HSO_5^- , similar to the analogous H_2O_2 system,¹⁴ is 2,6-dichloro-1,4-benzoquinone (DCBQ). In a series of stopped-flow experiments, the reaction was followed at the characteristic 395 nm Soret band of the catalyst. The reaction was complete well within 1 min but the disappearance of Fe^{III} TPPS became slower when the concentration of TCP was increased. This indicates that the substrate either inhibits the oxidation of the catalyst or regenerates it. The observations can be rationalized in terms of the following simple kinetic model



$$v_{10} = k_1^s [\text{Fe}^{\text{III}}\text{TPPS}] [\text{HSO}_5^-]$$



$$v_{11} = k_0 [\text{Int}_1] [\text{TCP}]$$



$$v_{12} = k_2^s [\text{Int}_1] [\text{HSO}_5^-]$$

Intermediate Int_1 , $(\text{TPPS}^+) \text{Fe}^{\text{IV}}=\text{O}$, is either reduced back to Fe^{III} TPPS by TCP or oxidized to Int_2 by the oxidant. The latter process irreversibly deactivates the catalyst.

The experimental kinetic traces could not be fitted to any of the explicit rate equations commonly used in reaction kinetics. The set of differential equations representing the kinetic model given in eqn (10)–(12) was solved numerically and a non-linear least-square fitting algorithm was used to find the best values of the fitted parameters.^{33,49} In these calculations, k_1^s and k_2^s were included with fixed values reported in the previous section of this paper, while rate constant k_0 and the molar absorbances of Int_1 and DCBQ were fitted. The following values were obtained for these parameters: $k_0 = (6.4 \pm 0.5) \times 10^6 \text{ M}^{-1} \text{ s}^{-1}$, $\epsilon(\text{Int}_1, 395 \text{ nm}) = (1.4 \pm 0.5) \times 10^4 \text{ M}^{-1} \text{ cm}^{-1}$, $\epsilon(\text{DCBQ}, 395 \text{ nm}) = (4.4 \pm 0.5) \times 10^3 \text{ M}^{-1} \text{ cm}^{-1}$. Fig. 9 shows two of the measured curves along with the best fit obtained. The excellent agreement of the experimental and calculated data demonstrates the validity of the model and lends strong support to the conclusions reached in this study.

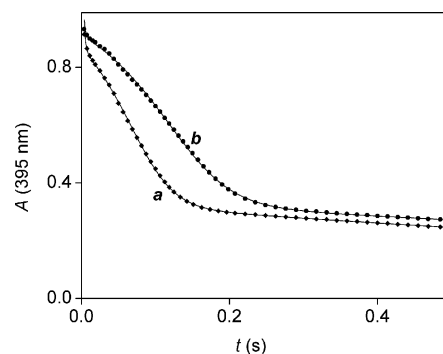


Fig. 9 Comparison of experimental (markers) and fitted (lines) kinetic traces during the reaction oxidation of 2,4,6-trichlorophenol with HSO_5^- catalyzed by Fe^{III} TPPS. $[\text{Fe}^{\text{III}}\text{TPPS}] = 6.9 \mu\text{M}$; $[\text{HSO}_5^-] = 4.9 \text{ mM}$; $[2,4,6\text{-trichlorophenol}] = 43 \mu\text{M}$ (a), $86 \mu\text{M}$ (b); $\text{pH} = 1.30$; $\lambda = 395 \text{ nm}$; optical path length = 1.00 cm; $T = 25.0 \text{ }^\circ\text{C}$; $I = 0.1 \text{ M}$ (NaClO_4); only a selection of measured points ($\sim 7\%$) is shown for clarity.

Earlier, we studied the Fe^{III} TPPS-catalyzed oxidation of TCP using H_2O_2 as the oxidant and proposed that the substrate is oxidized by an iron-containing steady-state intermediate (Cat'), which was assumed to be the hydroperoxo complex, $\text{TPPSFe}^{\text{III}}\text{-OOH}$.¹⁴ The comparison of these data¹⁴ with present results reveals an interesting point. The Fe^{III} TPPS-catalyzed oxidations of the same substrate by H_2O_2 and HSO_5^- proceed *via* slightly different mechanisms because Cat' cannot be the same as Int_1 identified in this work. First, steady-state kinetics clearly implied that the decomposition of Cat' is a first-order process that does not depend on the concentration of H_2O_2 ,¹⁴ whereas Int_1 is oxidized through a dominantly H_2O_2 -dependent pathway (k_{2a}^{H} and k_{2b}^{H} in Scheme 1). Second, the rate constants for both the oxidation of Int_1 (k_{2a}^{H} and k_{2b}^{H}) and the reaction between Int_1 and TCP (k_0) determined in this work seem too low for similar reactions of Cat' . For example, model calculations showed that k_{2b}^{H} should be greater than 10 s^{-1} for steady-state conditions to apply in the H_2O_2 oxidation if Cat' and Int_1 were the same. It seems likely that the catalytically most active intermediate in the H_2O_2 system (Cat') is $\text{TPPSFe}^{\text{III}}\text{-OOH}$ as postulated in our earlier work.¹⁴ This species is expected to form as an immediate product in the reaction of Fe^{III} TPPS with H_2O_2 (but not with HSO_5^-) and can undergo fast heterolytic O–O bond cleavage to give Int_1 , which is a detectable intermediate. Int_1 is not very important in the catalytic cycle in the presence of

H₂O₂ because it is a lot less reactive toward TCP than Cat', and its concentration is never as high as in the HSO₅⁻ system.

Conclusion

This study shows that studying the kinetics of the reaction between an oxidant and a catalyst without any oxidizable substrate is very important even when the primary objective is to explore the catalytic oxidation reaction. In the Fe^{III}TPPS–H₂O₂–chlorophenol system, the most active form of the catalyst is clearly not the same as the first spectroscopically detectable intermediate of the reaction in the absence of chlorophenol, which gives the general warning that isolated and spectroscopically or structurally characterized intermediates of a reaction may in fact have little relevance in catalytic cycles. Reactive species should not be identified solely based on spectral or structural studies, kinetic data are also essential.

Acknowledgements

The authors thank the Hungarian Science Foundation for financial support under grant No. F049498. Dr János Török and Mr Lajos Nagy are gratefully acknowledged for assistance in the ESI-MS measurements. GL wishes to thank the Hungarian Academy of Sciences for a Bolyai János Research Fellowship.

References

- 1 A. Sorokin, J. L. Séris and B. Meunier, *Science*, 1995, **268**, 1163–1166.
- 2 T. J. Collins, *Science*, 2001, **291**, 48–49.
- 3 T. J. Collins, *Acc. Chem. Res.*, 2002, **35**, 782–790.
- 4 S. Sen Gupta, M. Stadler, C. A. Noser, A. Ghosh, B. Steinhoff, D. Lenoir, C. P. Horwitz, K.-W. Schramm and T. J. Collins, *Science*, 2002, **296**, 326–328.
- 5 J. A. Kovacs, *Science*, 2003, **299**, 1024–1025.
- 6 J. U. Rohde, J. H. In, M. H. Lim, W. W. Brennessel, M. R. Bukowski, A. Stubna, E. Münck, W. Nam and L. Que, Jr., *Science*, 2003, **299**, 1037–1039.
- 7 J. T. Groves, *J. Inorg. Biochem.*, 2006, **100**, 434–447.
- 8 T. M. Makris, K. von Koenig, I. Schlichting and S. G. Sligar, *J. Inorg. Biochem.*, 2006, **100**, 507–518.
- 9 F. T. de Oliveira, A. Chanda, D. Banerjee, X. P. Shan, S. Mondal, L. Que, Jr., E. Bominaar, E. Münck and T. J. Collins, *Science*, 2007, **315**, 835–838.
- 10 B. J. Brazeau, R. N. Austin, C. Tarr, J. T. Groves and J. D. Lipscomb, *J. Am. Chem. Soc.*, 2001, **123**, 11831–11837.
- 11 L. G. Beauvais and S. J. Lippard, *J. Am. Chem. Soc.*, 2005, **127**, 7370–7378.
- 12 G. Lente and J. H. Espenson, *Chem. Commun.*, 2003, 1162–1163.
- 13 G. Lente and J. H. Espenson, *J. Photochem. Photobiol., A*, 2004, **163**, 249–258.
- 14 G. Lente and J. H. Espenson, *Int. J. Chem. Kinet.*, 2004, **36**, 449–455.
- 15 G. Lente and J. H. Espenson, *New J. Chem.*, 2004, **28**, 847–852.
- 16 G. Lente and J. H. Espenson, *Green Chem.*, 2005, **7**, 28–34.
- 17 T. G. Traylor and F. Xu, *J. Am. Chem. Soc.*, 1987, **109**, 6201–6202.
- 18 T. C. Bruice, P. N. Balasubramanian, R. W. Lee and J. R. L. Smith, *J. Am. Chem. Soc.*, 1988, **110**, 7890–7892.
- 19 G. Labat, J. L. Séris and B. Meunier, *Angew. Chem., Int. Ed. Engl.*, 1990, **29**, 1471–1473.
- 20 W. Nam, M. H. Lim, H. J. Lee and C. Kim, *J. Am. Chem. Soc.*, 2000, **122**, 6641–6647.
- 21 V. Lepentsiotis, R. van Eldik, F. F. Prinsloo and J. J. Pienaar, *J. Chem. Soc., Dalton Trans.*, 1999, 2759–2767.
- 22 T. K. Saha, S. Karmaker and K. Tamagake, *Luminescence*, 2003, **18**, 259–267.
- 23 N. A. Stephenson and A. T. Bell, *Inorg. Chem.*, 2007, **46**, 2278–2285.
- 24 E. B. Fleischer, J. M. Palmer, T. S. Srivastava and A. Chatterjee, *J. Am. Chem. Soc.*, 1971, **93**, 3162–3167.
- 25 A. A. El-Awady, P. C. Wilkins and R. G. Wilkins, *Inorg. Chem.*, 1985, **24**, 2053–2057.
- 26 J. T. Groves and Y. Watanabe, *J. Am. Chem. Soc.*, 1988, **110**, 8443–8452.
- 27 J. T. Groves, Z. Gross and M. K. Stern, *Inorg. Chem.*, 1994, **33**, 5065–5072.
- 28 G. Gordon and P. Tewari, *J. Phys. Chem.*, 1966, **60**, 200–204.
- 29 B. Tonomura, H. Nakatani, M. Ohnishi, J. Yamaguchi-Ito and K. Hiromi, *Anal. Biochem.*, 1978, **84**, 370–383.
- 30 G. Peintler, A. Nagy, A. K. Horváth, T. Körtvélyesi and I. Nagypál, *Phys. Chem. Chem. Phys.*, 2000, **2**, 2575–2586.
- 31 H. M. Irving, M. G. Miles and L. D. Pettitt, *Anal. Chim. Acta*, 1967, **38**, 475–488.
- 32 *SCIENTIST, version 2.0*, Micromath Software, Salt Lake City, UT, USA, 1995.
- 33 G. Peintler, *ZiTa, version 4.1*, Attila József University, Szeged, Hungary, 1997.
- 34 *MatLab for Windows, version 4.2c1*, The Mathworks, Inc., Natick, MA, USA, 1994.
- 35 J. H. Espenson, in *Chemical Kinetics and Reaction Mechanisms*, McGraw-Hill, New York, 2nd edn, 1995.
- 36 I. Kerezi, G. Lente and I. Fábián, *J. Am. Chem. Soc.*, 2005, **127**, 4785–4793.
- 37 I. Kerezi, G. Lente and I. Fábián, *Dalton Trans.*, 2006, 955–960.
- 38 D. M. Stanbury and J. N. Figlar, *Coord. Chem. Rev.*, 1999, **187**, 223–232.
- 39 M. Galajda, G. Lente and I. Fábián, *J. Am. Chem. Soc.*, 2007, **129**, 7738–7739.
- 40 I. Hamachi, S. Tsukiji, S. Shinkai and S. Oishi, *J. Am. Chem. Soc.*, 1999, **121**, 5500–5506.
- 41 J. Premkumar and R. Ramaraj, *J. Mol. Catal. A: Chem.*, 1999, **142**, 153–162.
- 42 M. Weitzer, M. Schatz, F. Hampel, F. W. Heinemann and S. Schindler, *J. Chem. Soc., Dalton Trans.*, 2002, 686–694.
- 43 L. Stryer, in *Biochemistry*, W. H. Freeman & Co., New York, 4th edn, 1995.
- 44 E. L. Wehry and L. B. Rogers, *J. Am. Chem. Soc.*, 1966, **88**, 351–354.
- 45 J. Terner, V. Palaniappan, A. Gold, R. Weiss, M. M. Fitzgerald, A. M. Sullivan and C. M. Hosten, *J. Inorg. Biochem.*, 2006, **100**, 480–501.
- 46 Z. Z. Pan, R. Zhang and M. Newcomb, *J. Inorg. Biochem.*, 2006, **100**, 524–532.
- 47 D. Kumar, S. P. de Visser and S. Shaik, *J. Am. Chem. Soc.*, 2005, **127**, 8204–8213.
- 48 T. Kamachi and K. Yoshizawa, *J. Am. Chem. Soc.*, 2005, **127**, 10686–10692.
- 49 G. Lente and I. Fábián, *J. Chem. Soc., Dalton Trans.*, 2002, 778–784.